The American Journal of Pathology, Vol. 180, No. 4, April 2012
Copyright © 2012 American Society for Investigative Pathology.
Published by Elsevier Inc. All rights reserved.
DOI: 10.1016/j.ajpath.2011.12.017

Short Communication

Negative Feedback Mechanisms Surpass the Effect of Intrinsic EGFR Activation during Skin Chemical Carcinogenesis

Maik Dahlhoff,* Christian Rose,† Martin Hrabé de Angelis,‡§ Eckhard Wolf,* and Marlon R. Schneider*

From the Institute of Molecular Animal Breeding and Biotechnology and the Laboratory for Functional Genome Analysis, Gene Center, LMU Munich, Munich; the Department of Dermatology,† University Hospital Schleswig-Holstein, University of Lübeck, Lübeck; the Institute of Experimental Genetics,‡ Helmholtz Zentrum München, German Research Center for Environmental Health (GmbH), Neuherberg; and the Institute of Experimental Genetics,§ Technical University of Munich, Munich, Germany*

The negative feedback regulation of epidermal growth factor receptor (EGFR) and other tyrosine kinase receptors, including receptor dephosphorylation and endocytosis followed by degradation, is becoming recognized as a major determinant of receptor function. To evaluate the significance of the negative regulation of EGFR during carcinogenesis *in vivo*, we subjected the mutant mouse line Dsk5, in which the intrinsic activation of the receptor due to a point mutation is normally counterbalanced by increased posttranslational receptor down-regulation, to skin chemical carcinogenesis. Dsk5 mice showed reduced tumor numbers and tumor burden compared with control littermates, and Dsk5-derived tumors showed a reduction in the activation and total levels of EGFR. Furthermore, the transcript levels of several molecules known to act as negative regulators of EGFR were significantly increased in Dsk5-derived tumors. Another intriguing observation was the appearance of tumors with sebaceous differentiation in the ears of Dsk5 mice after chemical carcinogenesis. Further studies are necessary to reveal whether these tumors represent a cell type–specific evasion from EGFR negative feedback machinery. In conclusion, this study reveals that several negative feedback regulators contribute to suppression of the intrinsic activation of mutant EGFR during skin carcinogenesis, stressing the potential exploitation of negative regulators as either therapeutic targets or diagnostic tools in cancer and other diseases. ***(Am J Pathol 2012, 180: 1378–1385; DOI: 10.1016/j.ajpath.2011.12.017)***

The epidermal growth factor receptor (EGFR) system exerts multiple actions during development in adult tissue homeostasis and in diseases such as cancer.[1–4] These actions are predominantly the result of forward signaling by proteins composing numerous signaling cascades and immediate early genes encoding transcription factors. Recently, negative feedback (or inhibitory feedback) regulation of EGFR and other receptor tyrosine kinases, including receptor dephosphorylation and endocytosis followed by degradation, has become recognized as a major determinant of receptor signaling outcome.[5,6] In accordance with their role in negative regulation of cell signaling, components of negative feedback pathways are often down-regulated in certain tumor types, with obvious clinical relevance. A particularly illustrative example is a phase I clinical trial of rapamycin, an inhibitor of the mammalian target of rapamycin, in patients with recurrent phosphatase and tensin homolog–deficient glioblastoma.[7] Also, EGFR mutations characterized by basal, ligand-independent receptor activation that is sufficient to initiate downstream pathways but not strong enough to recruit signal transduction protein CBL-C (CBLC) to trigger receptor ubiquitinylation and subsequent degradation are frequently observed in lung cancer cells.[8] Thus, from a pathologic perspective, negative feedback regulation of receptor activity is likely to become an important factor for evaluating disease resistance to new drugs or for determining specific drug combinations.

Supported by the Deutsche Forschungsgemeinschaft (SCHN 1081/3-1).

Accepted for publication December 22, 2011.

Supplemental material for this article can be found at *http://ajp.amjpathol.org* or at doi: 10.1016/j.ajpath.2011.12.017.

Address reprint requests to Marlon R. Schneider, D.V.M., Gene Center, LMU Munich, Feodor-Lynen-Str. 25, 81377, Munich, Germany. E-mail: schnder@lmb.uni-muenchen.de.

The skin is one of the tissues in which EGFR signaling is of prominent importance, and its deregulation is associated with several diseases, such as cancer, psoriasis, and defective wound healing.[9] The N-ethyl-N-nitrosourea–induced Dsk5 mutation, recovered because affected mice displayed increased skin pigmentation, is characterized by a T→A transversion in the kinase domain of the *Egfr* gene leading to a Leu→Gln substitution.[10] The mutation results in a considerable increase in basal EGFR signaling (estimated to be 5- to 10-fold higher than normal in *in vitro* studies) with a concomitant reduction in EGFR steady state protein levels.[10] In fact, the posttranslational EGFR down-regulation probably explains the mild phenotype of the mice since such a high increase in EGFR activity would most likely immediately affect the health of mutant animals in different ways. For example, targeted overexpression of the EGFR ligand transforming growth factor-α in the skin of transgenic mice induces epidermal thickening and the development of papillomas,[11,12] overexpression of the ligand amphiregulin results in psoriatic lesions,[13,14] and ubiquitous overexpression of the EGFR ligand epigen causes epidermal thickening and highly enlarged sebaceous glands.[15] Thus, the dynamic balance between EGFR forward signaling derived from the mutation and its extensive compensation by negative feedback mechanisms observed in Dsk5 mice seems to be a suitable model for studying EGFR negative feedback regulation.

Herein, we asked whether a perturbation in this balance, brought about by tumorigenesis, would result in a hypermorphic or hypomorphic phenotype, reflecting enhanced or reduced EGFR activity. For this purpose, we used skin multistage chemical carcinogenesis, a widely used model involving initiation of epidermal keratinocytes by a genotoxic chemical followed by repeated promotion stimuli.[16,17]

Materials and Methods

Animals

Dsk5 mice were donated by the Helmholtz Zentrum München, German Research Center for Environmental Health (GmbH) (Neuherberg, Germany). The animals were maintained in the C57BL/6N background under specific pathogen-free conditions in a closed barrier facility with free access to a standard rodent diet and water. Tail tip DNA was used for genotyping by PCR as previously described.[10] All the experiments were approved by the local veterinary authority (Committee on Animal Health and Care of the local governmental body of the State of Upper Bavaria) and were performed according to the German Animal Welfare Act.

Chemical Carcinogenesis and Tissue Processing

Chemical carcinogenesis was performed according to internationally accepted standards.[17] In experiment I, 7-week-old Dsk5 females and control littermates were shaved on their backs and received a single application (400 nmol) of the initiating agent 7,12-dimethylbenz(a)anthracene (DMBA; Sigma-Aldrich Chemie GmbH, Munich, Germany). This was followed by multiple applications (twice per week, 10 nmol each) of the promoting agent 12-O-tetradecanoylphorbol-13-acetate (TPA; Sigma-Aldrich Chemie GmbH) for 24 weeks; the mice were then euthanized (Figure 1A). The design of experiment II was the same as that of experiment I (Figure 1A) but without applications of TPA. All the mice were examined every week for the development of papillomas. After euthanasia, tumors and skin samples were fixed in 4% paraformaldehyde (Sigma-Aldrich Chemie GmbH), dehydrated, and embedded in paraffin or snap frozen and stored at −80°C.

Immunohistochemical and Histologic Analyses

H&E-stained sections were used for histopathologic analysis. For the detection of proliferating cells, immunohistochemical staining of Ki-67 was performed. Briefly, sections were boiled for antigen retrieval in 10 mmol/L sodium citrate buffer (pH 6.0), and the endogenous peroxidase was blocked with 3% H_2O_2 for 15 minutes. Slides were blocked with 5% rabbit serum and were incubated overnight at 4°C with a rat anti–Ki-67 antibody (Dako Denmark A/S, Glostrup, Denmark) diluted 1:200. After washing in Tris-buffered saline solution, the slides were incubated for 1 hour with a secondary biotin-conjugated rabbit anti-rat antibody (Dako Denmark A/S) diluted 1:200 and then for 30 minutes with streptavidin-biotin complex. 3,3′-diaminobenzidine (Kem-En-Tec Diagnostics A/S, Taastrup, Denmark) was used as chromogen. The procedure for immunohistochemical analysis against perilipin 2 was similar to that for Ki-67 staining using guinea pig anti-perilipin 2 antibody (Progen Biotechnik GmbH, Heidelberg, Germany) diluted 1:250 and rabbit anti-guinea pig (Dako Denmark A/S) diluted 1:250 as secondary antibody.

For the quantitative evaluation of sebaceous gland area and proliferation index, three different sections from each ear of 6-month-old control ($n = 4$) and Dsk5 ($n = 5$) females that never received DMBA or TPA treatment were H&E stained. Pictures covering a length of 4.33 mm of epidermis were taken using a ×200 magnification lens and a Leica DFC425C digital camera (Leica Microsystems GmbH, Wetzlar, Germany), resulting in a total length of 26 mm of ear skin per animal to be measured. The area of all visible sebaceous glands was recorded using LAS Software version 3.8.0 (Leica Microsystems GmbH) and was used to calculate the mean gland area. For determining the proliferation index, the total number of cells and the number of proliferating cells per sebaceous gland were determined on the same samples after staining for Ki-67.

Analysis of the Hras1 Mutation

Genomic DNA was isolated from tail skin, back tumors, and ear tumors. Detection of the *Hras1* mutation was performed as described previously.[18] The PCR product flanking the mutations was digested with the restriction

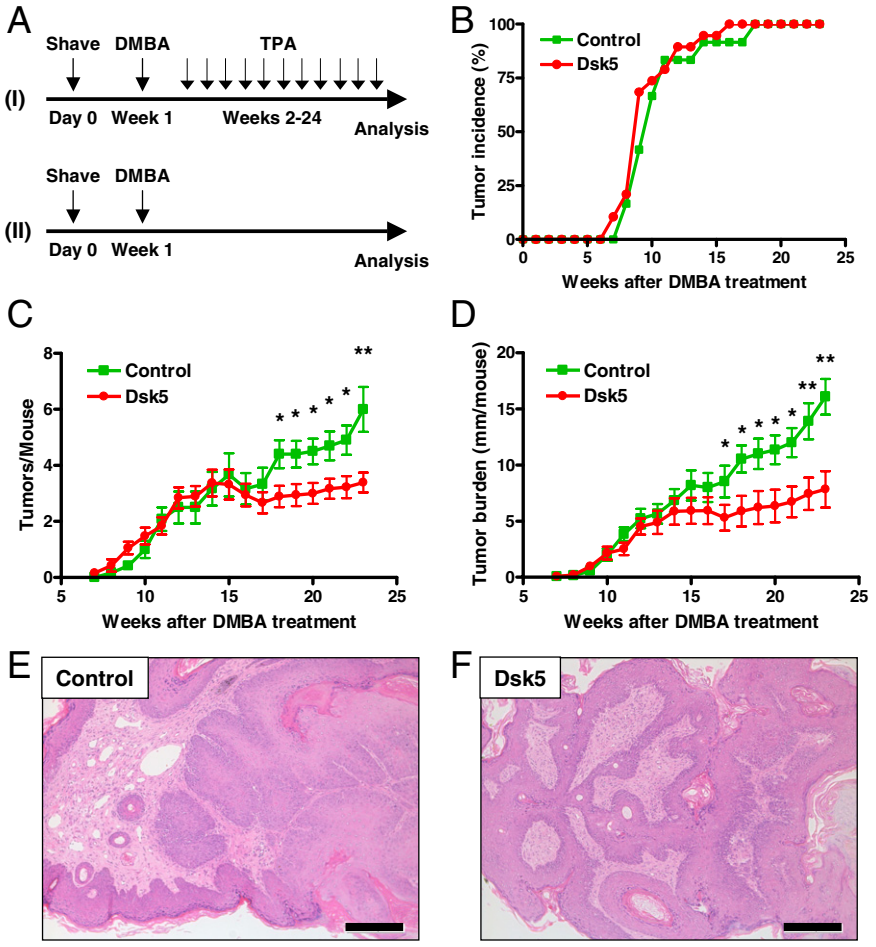

Figure 1. Tumor growth is significantly reduced in Dsk5 mice after multistage chemical carcinogenesis. **A:** Schematic representation of the protocols for chemical carcinogenesis used in Experiments I and II. **B:** Evaluation of the tumor incidence revealed no differences between groups. **C:** Tumor numbers are significantly reduced in Dsk5 mice compared with control littermates (group × time: $P < 0.0001$). **D:** The tumor burden is significantly reduced in Dsk5 mice (group × time: $P < 0.0001$). Histologic analysis of H&E-stained sections revealed no differences in tumor morphologic features between control (**E**) and Dsk5 (**F**) mice. Data are mean ± SEM; 12 control and 19 Dsk5 mice per group. $^{*}P < 0.05$, $^{**}P < 0.01$ by Student's *t*-test. Scale bars: 200 μm.

enzyme XbaI at 37°C for 3 hours. The digest was electrophoresed on a 3% high-resolution agarose gel (Sigma-Aldrich Chemie GmbH).

Western Blot Analysis

The Western blot experiments have been described in detail elsewhere.[19] Briefly, samples were homogenized in extraction buffer, and equal amounts of protein were electrophoresed on 12% polyacrylamide-SDS gels and then blotted to polyvinylidene difluoride membranes (GE Healthcare, Munich, Germany). Incubation with primary antibodies was performed overnight at 4°C. The following antibodies, diluted in 5% dry milk, were used: goat anti–phospho-EGFR Tyr 1173 (1:250; #sc-12351; Santa Cruz Biotechnology, Santa Cruz, CA), rabbit anti-EGFR (1:500; #sc-03; Santa Cruz Biotechnology), rabbit anti-HGS (1:500; #sc-30221; Santa Cruz Biotechnology), rabbit anti-LRIG1 (1:500; #sc-134435; Santa Cruz Biotechnology), and rabbit anti–α-tubulin (1:5000; #2125; Cell Signaling Technology Inc., Beverly, MA). Appropriate horseradish peroxidase–conjugated secondary antibodies were used. Immunoreactive bands were visualized by chemiluminescence using an ECL kit (GE Healthcare). Band intensities were quantified using the ImageQuant software package version 5.0 (Molecular Dynamics, Krefeld, Germany).

Quantitative RT-PCR

Tumors were homogenized in TRIzol (Invitrogen, Karlsruhe, Germany) for RNA isolation. RNA samples, 5 μg, were reverse transcribed in a final volume of 35 μL using SuperScript II Reverse Transcriptase (Invitrogen) according to the manufacturer's instructions. Quantitative mRNA expression analysis was performed by real-time quantitative RT-PCR (RT-qPCR) using the LightCycler 480 System and the LightCycler 480 Probes Master (Roche Diagnostics GmbH, Penzberg, Germany). The final primer concentration was 0.5 μmol/L, and the probe concentration was 0.2 μmol/L. The final reaction volume was 10 μL, and cycle conditions were 95°C for 5 minutes for the first cycle, followed by 45 cycles of 95°C for 10 seconds, 60°C for 15 seconds, and 72°C for 1 second. Quantitative values were obtained from the C_T number at which the increase in the signal associated with the exponential growth of PCR products begins to be detected. Transcript copy numbers were normalized to Actb mRNA copies. Results are expressed as fold differences in target gene expression relative to *Actb* transcripts. The ΔC_T value of the sample was determined by subtracting the average C_T value of the target gene from the average C_T value of the *Actb* gene. Probes were labeled with the reporter dye FAM at the 5′ end and with the quencher dye TAMRA at the 3′ end. For each primer pair, we

Table 1. Sequences of the Primers and Probes Used for RT-qPCR Analysis

ACTB	
Forward primer	5′-CGTGAAAAGATGACCCAGATCA-3′
Reverse primer	5′-CACAGCCTGGATGGCTACGT-3′
Fluorogenic probe	5′-TTTGAGACCTTCAACACCCCAGCCA-3′
PTPRK	
Forward primer	5′-TCCTTGCGATAAATCTCCTCA-3′
Reverse primer	5′-TCTGCCCAGCATTGACCT-3′
Fluorogenic probe	5′-TGGTGATG-3′
PTPN1	
Forward primer	5′-GGGCCCTTTACCAAACACA-3′
Reverse primer	5′-CTGCTCTTCTGCTCCCACA-3′
Fluorogenic probe	5′-CTGGGAGA-3′
PTPRJ	
Forward primer	5′-TGAACATCAGTGCCTCAAGC-3′
Reverse primer	5′-TACGGGACCCATCGTAATTG-3′
Fluorogenic probe	5′-GACCTGGA-3′
ERRFI1	
Forward primer	5′-CTGTTGTAGCAAGAGGCTTTCA-3′
Reverse primer	5′-TCAGACCCCAAACACTGATG-3′
Fluorogenic probe	5′-GCAGTGGA-3′
CBLC	
Forward primer	5′-CCTGTACCAGCTCACCAAGG-3′
Reverse primer	5′-GAAGCACGCACCGAACTC-3′
Fluorogenic probe	5′-GGAGGCAG-3′
NEDD8	
Forward primer	5′-TGCTAATTAAAGTGAAGACGCTGA-3′
Reverse primer	5′-TTGTCTGTGGGTTCGATGTC-3′
Fluorogenic probe	5′-GGAAGGAG-3′
LRIG1	
Forward primer	5′-GCCTTCTCCTACGTTAGCTTCA-3′
Reverse primer	5′-TCAGTAGATATGGCGTCTTCCA-3′
Fluorogenic probe	5′-CAGCCAG-3′
HGS	
Forward primer	5′-CTTCTGTGGCAAGTGCTCCT-3′
Reverse primer	5′-TCCTTCTCAATGCCGAACTT-3′
Fluorogenic probe	5′-CTCCACCA-3′
STAMBP	
Forward primer	5′-GCCTTTGAGGAGATGATCCA-3′
Reverse primer	5′-TTGAACAATTTTCAGCCGTTC-3′
Fluorogenic probe	5′-AGGAGCTG-3′
USP8	
Forward primer	5′-CTGAAATGGCTCCTTCGTCT-3′
Reverse primer	5′-CTGGGGCTTGACTTTGTGAG-3′
Fluorogenic probe	5′-GGAAGGAG-3′

performed no-template control and no-RT control assays, which produced negligible signals that were usually >40 in C_T value. Experiments were performed in duplicate for each sample. Sequences of the primers (Thermo Fisher Scientific, Schwerte, Germany) and probes (Roche Diagnostics GmbH) for the target transcripts are given in Table 1.

Statistical Analysis

Data on the number of tumors per mouse and tumor burden were statistically evaluated by analysis of variance (PROC MIXED; SAS, release 8.2; SAS Institute, Inc., Cary, NC), taking the fixed effects of group (Dsk5 or control), time (relative to tumor initiation), and the group × time interaction as well as the random effect of animal into account. Differences in the numbers of tumors per mouse and in the tumor burden between Dsk5 and control mice for each time point were additionally tested for significance using a Student's *t*-test (GraphPad Prism version 5; GraphPad Software Inc., San Diego, CA). Differences in tumor-free lifetime were evaluated using Kaplan-Meyer survival analysis (SPSS, version 18.0; SPSS Inc., Chicago, IL). χ^2 tests were used to test differences in tumor incidence between groups at specific time points. RT-qPCR values were related to the mean value of the control group and were compared by Mann-Whitney *U*-tests (GraphPad Prism). Data are presented as mean ± SEM (tumors per mouse and tumor burden) or as box plots with medians (RT-qPCR). Densitometric data from Western blot analysis using four back skin or three tumor samples per group and the proliferation index ($n = 4$ mice per group) were analyzed using Student's *t*-test. $P < 0.05$ was considered significant.

Results

Dsk5 Mice Show Impaired Tumor Development despite Intrinsic EGFR Activation

In experiment I, including a single DMBA application followed by repeated administration of TPA (Figure 1A), tumors became visible on the backs of Dsk5 ($n = 19$) and control ($n = 12$) mice from weeks 6 to 7 after DMBA treatment, and the proportion of tumor-bearing mice did not differ between groups over time (Figure 1B; $P = 0.405$). The number of tumors per mouse (Figure 1C) increased significantly with time in both groups (effect of time: $P < 0.0001$), but the number of tumors was significantly lower in Dsk5 mice than in controls over time (effect of group × time: $P < 0.0001$). This difference was reflected in a significantly lower tumor burden (Figure 1D) in Dsk5 mice compared with controls (effect of group: $P = 0.0169$; effect of group × time: $P < 0.0001$). Histologic evaluation of H&E-stained sections of Dsk5 and control back skin tumors revealed typical papillomas with well-bordered basement membranes and surrounded by hyperplastic epidermis with orthologous keratosis (Figure 1, E and F).

Since this rather surprising result was not predictable at the beginning of the investigation, a separate experiment (II) was initiated to evaluate the ability of the Dsk5 mutation to facilitate tumor progression without TPA treatment (Figure 1A). For this purpose, Dsk5 ($n = 11$) and control ($n = 8$) females received a single application (400 nmol) of the initiating agent DMBA without further applications of TPA. Back skin tumor development was never observed in any mouse independent of the genotype.

Multiple Negative Feedback Mechanisms Blunt the Intrinsic Activation of EGFR in Tumors

The intrinsic activation of EGFR due to the Dsk5 mutation has been reported to cause posttranslational down-regulation of the receptor in liver cells.[10] Western blot analysis confirmed increased phosphorylation of EGFR in the back skin of untreated Dsk5 mice compared with control littermates, whereas a reduction in total EGFR, as reported for liver cells, was not evident (Figure 2A; see also Supplemental Figure S1A at *http://ajp.amjpathol.org*).

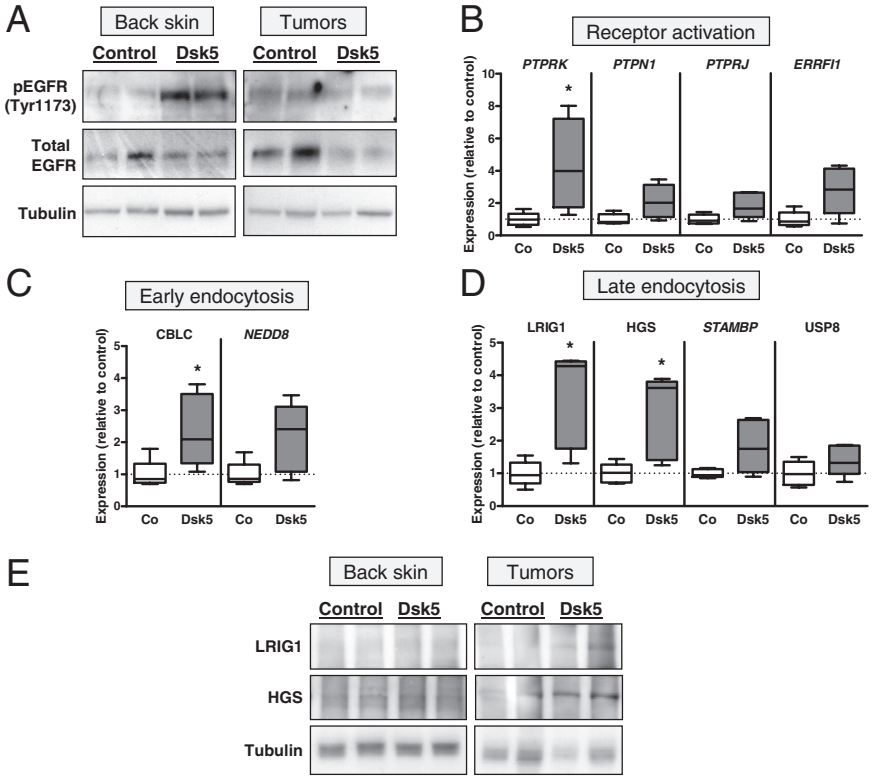

Figure 2. A: Detection of phospho-EGFR (p-EGFR), total EGFR, and tubulin in normal back skin and tumors from Dsk5 mice and control littermates by Western blot analysis. **B–D:** Quantification of the transcript levels of negative feedback molecules for receptor activation (**B**), early endocytosis (**C**), and late endocytosis (**D**) in tumors by RT-qPCR (expressed as changes relative to controls). $^*P < 0.05$ by Mann-Whitney *U*-test. Co, control. **E:** Detection of LRIG1, HGS, and tubulin in normal back skin and tumors from Dsk5 mice and control littermates by Western blot analysis. *PTPRK*, protein tyrosine phosphatase, receptor type, K; *PTPN1*, protein tyrosine phosphatase, nonreceptor type 1; *PTPRJ*, protein tyrosine phosphatase, receptor type, J; *ERRFI1*, ERBB receptor feedback inhibitor 1; *NEDD8*, neural precursor cell expressed, developmentally down-regulated 8; *STAMBP*, STAM binding protein; *USP8*, ubiquitin-specific peptidase 8.

Analysis of the tumors, in contrast, did not show an increase in EGFR phosphorylation in samples from Dsk5 mice (Figure 2A). Although densitometric analysis revealed increased EGFR phosphorylation in Dsk5 tumors when normalized to total receptor levels (see Supplemental Figure S1A at *http://ajp.amjpathol.org*), this finding results from the remarkable reduction in the levels of total EGFR compared with control tumors (Figure 2A; see also Supplemental Figure S1A at *http://ajp.amjpathol.org*). Accordingly, EGFR phosphorylation is significantly increased in Dsk5 back skin but is unchanged in Dsk5 tumors compared with in control samples when expressed as a ratio of tubulin levels (see Supplemental Figure S1A at *http://ajp.amjpathol.org*).

In an attempt to identify the specific mechanisms and molecules involved in the suppression of EGFR activity in tumors, we evaluated the levels of several known negative regulators of tyrosine kinase receptor signaling by RT-qPCR. We adopted the nomenclature put forward by Avraham and Yarden[6] and evaluated molecules in the following categories: receptor activation (four transcripts), early receptor endocytosis (two transcripts), and late receptor endocytosis (four transcripts). As shown in Figure 2B, the levels of all examined transcripts tended to be higher in Dsk5 tumors, with statistical significance detected for *Ptprk*. The same tendency was observed in the categories of early (Figure 2C) and late (Figure 2D) receptor endocytosis, with significantly higher transcript levels of *Cblc*, *Lrig1,* and *Hgs* in Dsk5 tumors than in controls. Next, using as a criterion the RT-qPCR results and the availability of reliable antibodies, we evaluated the protein levels of a subset of these molecules by Western blot analysis. Although no difference between groups was observed for CBLC and NEDD8 (data not shown), we detected increased leucine-rich repeats and Ig-like domains protein 1 (LRIG1) and hepatocyte growth factor–regulated tyrosine kinase substrate (HGS) protein levels in Dsk5 tumors compared with in tumors from control mice (Figure 2E; see also Supplemental Figure S1B at *http://ajp.amjpathol.org*).

Growth of Sebaceous Adenomas in the Ears of Dsk5 Mice

In addition to the tumors observed on the backs of the mice in experiment I, small papillomas were observed on the ears of Dsk5 mice starting 17 weeks after DMBA application (Figure 3A). At the end of the experiment, ~60% of the females (11 of 19) showed at least one ear tumor, whereas tumors at this site were never observed in control females. Histologic analysis of H&E-stained sections revealed an array of well differentiated sebaceous glands in every ear tumor analyzed (Figure 3B), and the presence of lipid-laden sebocytes was confirmed by the detection of the lipid droplet–associated protein perilipin 2 (Figure 3C). Ki-67 staining revealed that cells at the basal layer of the sebaceous gland acini were highly proliferative (Figure 3D). Since basal (undifferentiated) sebocytes were restricted to a single peripheral cell layer, these tumors were classified as cases of sebaceous hyperplasia.[20] A similarly high proportion of ear sebaceous hyperplasia was observed in Dsk5 mice (~80%, 9 of 11 females) treated with only DMBA (exper-

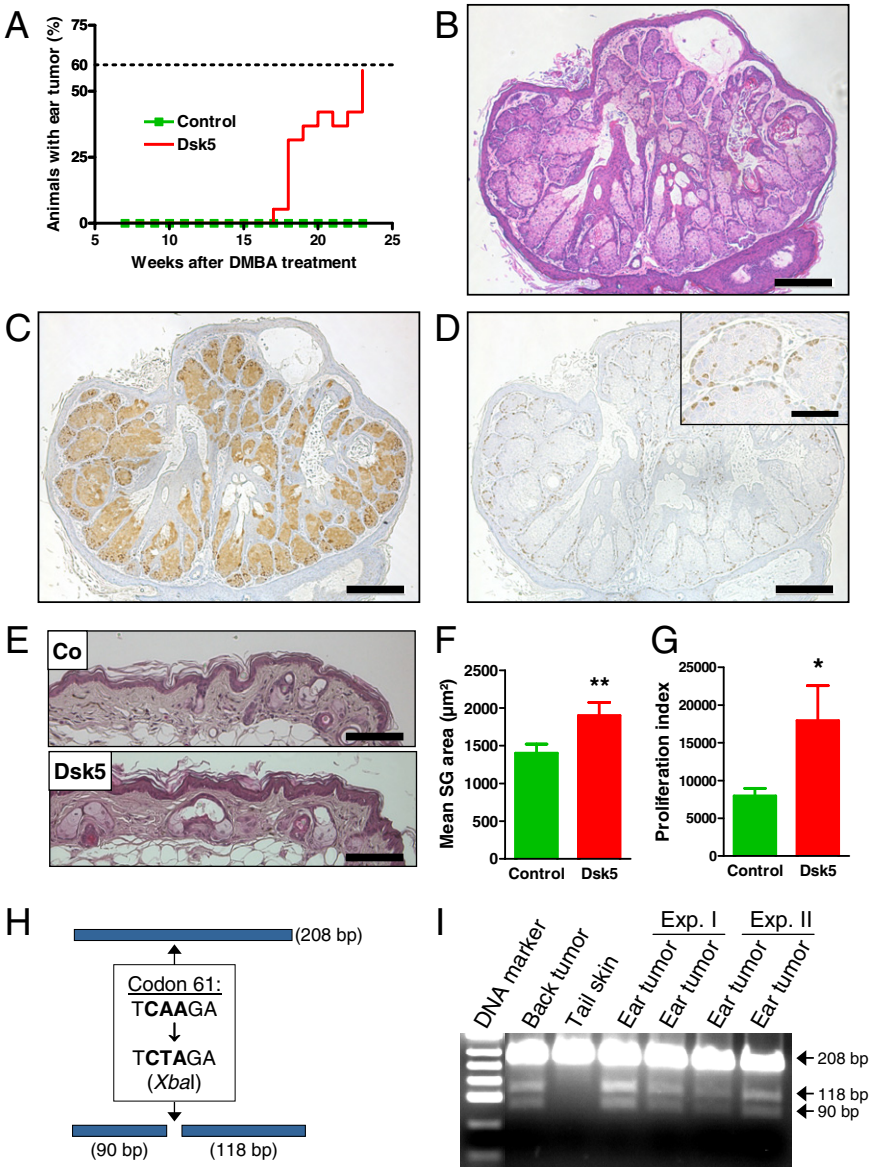

Figure 3. Development of sebaceous hyperplasia in the ears of Dsk5 mice. **A:** Time course of ear tumor growth in Dsk5 females and control littermates from experiment I. **B:** H&E-stained sections of ear tumors showed well differentiated acinolobular glandular formations consisting of cells with a typical foamy cytoplasm and small round nuclei. **C:** The tumors are perilipin 2 positive, confirming their sebaceous nature. **D:** Ki-67 staining demonstrated high proliferative activity in the cells at the periphery of the acini. **E:** Representative H&E-stained ear skin sections from 6-month-old control (Co) and Dsk5 mice that never received DMBA or TPA. **F:** Quantitative evaluation of the mean area of sebaceous glands (SGs) in the ear skin of control and Dsk5 mice. **G:** Quantitative evaluation of the proliferation index (Ki-67–positive nuclei/10^5 nuclei) of SGs in the ear skin of control and Dsk5 mice. Data are mean ± SD; four control and five Dsk5 mice per group. $^*P < 0.05$, $^{**}P < 0.01$ by Student's *t*-test. **H:** The underlying principle of the strategy used to detect the DMBA-induced *Hras* codon 61 mutation. A 208-bp fragment flanking the *Hras* codon 61 was amplified by PCR and subjected to an XbaI digest to detect the A→T transversion. **I:** The *Hras* mutation is present in ear sebaceous hyperplasia derived from experiments (Exp.) I and II. A back skin papilloma and tail skin are included as positive and negative controls, respectively. Scale bars: 200 µm (**B–D**); 50 µm (**inset** of **D**); and 100 µmol/L (**E**).

iment II), but, again, no ear tumors were detected in control females.

To evaluate whether a change in sebaceous gland morphologic features may be the underlying reason for the DMBA-induced sebaceous hyperplasia in Dsk5 mice, we assessed H&E-stained ear skin sections. Although no noticeable differences in sebaceous gland morphologic features were detected, the glands of Dsk5 mice tended to be larger than those of control mice (Figure 3E). Quantitative analysis confirmed this impression and revealed a statistically significant increase in the mean sebaceous gland area on the ears of Dsk5 females (Figure 3F). Also, quantitative evaluation of Ki-67–positive cells revealed a significant increase in the proliferation index of Dsk5 ear sebaceous glands compared with the ears of control littermates (Figure 3G; see also Supplemental Figure S1C at *http://ajp.amjpathol.org*).

To test whether the ear sebaceous hyperplasia is derived from cells carrying the DMBA-induced *Hras* mutation, we analyzed the typical A→T transversion at the second position of *Hras1* codon 61 (Figure 3H) by PCR and restriction fragment length polymorphism analysis. The *Hras* mutation was detected in every Dsk5 ear sebaceous hyperplasia entity analyzed in experiments I and II (Figure 3I).

Discussion

Herein, we used the N-ethyl-N-nitrosourea-induced–mutant mouse line Dsk5 to investigate whether the dynamic balance between increased intrinsic EGFR forward signaling derived from a point mutation and its extensive compensation by negative feedback mechanisms would become disrupted during multistage skin chemical carcinogenesis. To our surprise, the tumor number and the tumor burden in Dsk5 mice were significantly reduced compared with those in control littermates, suggesting

that the negative feedback mechanisms surpass the intrinsic activation of the receptor. In addition, Western blot analysis revealed that Dsk5 tumors show unchanged activation of EGFR concomitantly with a clear reduction in total EGFR protein levels. This is in contrast to the situation in normal Dsk5 skin samples, in which strong intrinsic activation of EGFR in the absence of down-regulation of total EGFR was observed. This tissue- or cell type–specific difference may explain why several phenotypical skin alterations (including hyperkeratosis, epidermal thickening, and increased skin pigmentation) but no alterations in the liver of Dsk5 mice have been reported.[10]

RT-qPCR revealed a significant increase in the transcript levels of several molecules known to act as negative regulators of EGFR, including receptor-type tyrosine-protein phosphatase kappa (PTPRK), a membrane protein previously reported to dephosphorylate EGFR in human keratinocytes,[21] CBLC, an early mediator of EGFR ubiquitin-dependent sorting and subsequent lysosomal and proteosomal degradation,[22] and two late stimulators of EGFR endocytosis: HGS[23] and LRIG1.[24,25] Some additional molecules, such as tyrosine-protein phosphatase non-receptor type 1 ($P = 0.056$) and STAM-binding protein ($P = 0.093$), showed an increase of expression in Dsk5 tumors close to statistical significance, indicating that further molecules are likely to be involved in the suppression of EGFR function in Dsk5 mice. Western blot analysis confirmed up-regulation of LRIG1 and HGS at the protein level.

An additional observation during these studies was the appearance of tumors with sebaceous differentiation in the ears of Dsk5 mice following both protocols of chemical carcinogenesis (spontaneous tumors of any kind were never observed). These tumors carried the typical DMBA-induced A→T transversion at the second position of *Hras* codon 61. Sebaceous neoplasias include a broad spectrum of lesions ranging from benign to highly malignant.[20] The tumors observed in the ears of Dsk5 mice were classified as sebaceous hyperplasia because they appeared as an array of well-differentiated sebaceous lobules with no more than two layers of peripheral undifferentiated cells. The proportion of undifferentiated basal cells and mature sebocytes in the acini is often used as a criterion to distinguish among sebaceous hyperplasia, sebaceous adenoma, and sebaceoma.[20] In humans, sebaceous hyperplasia exists in several forms and localizations, but its cause remains enigmatic.[20] Whereas papillomas with a sebaceous component are commonly detected after chemical carcinogenesis of the skin,[26,27] the massive and dominant presence of sebaceous hyperplasia as observed in Dsk5 mice is rather unusual. However, there are reports of similar lesions after application of the strong irritant tetradecane in rabbits[28] or after a high dose of DMBA in mice.[29] Although the researchers classified the tumors as sebaceous adenoma, the latter study included features resembling the present study, such as the appearance of tumors at sites distant from the application spot of the initiator and no requirement of promotion by TPA.[29] Further studies are necessary to clarify the specific pathways responsible for the development of sebaceous hyperplasia in DMBA-treated Dsk5 mice and whether this effect represents a cell type–specific evasion from the EGFR inhibitory feedback machinery. Quantitative evaluation revealed a significant increase in the area and in the proliferation index of sebaceous glands of Dsk5 females never treated with DMBA or TPA, suggesting that the availability of a larger number of putatively responsive cells may be a factor contributing to this intriguing phenotype.

In conclusion, this *in vivo* study reveals that several negative feedback regulators contribute to suppress the intrinsic activation of mutant EGFR during skin carcinogenesis. These results highlight the potential exploitation of receptor tyrosine kinase–negative regulators as therapeutic targets or as diagnostic tools in cancer and other diseases.

Acknowledgments

We thank Dr. Ingrid Renner-Müller and Petra Renner for excellent animal care and Stefanie Riesemann and Josef Millauer for assistance with mouse genotyping and Western blot analysis.

References

1. Yarden Y, Sliwkowski MX: Untangling the ErbB signalling network. Nat Rev Mol Cell Biol 2001, 2:127–137
2. Holbro T, Hynes NE: ErbB receptors: directing key signaling networks throughout life. Annu Rev Pharmacol Toxicol 2004, 44:195–217
3. Citri A, Yarden Y: EGF-ERBB signalling: towards the systems level. Nat Rev Mol Cell Biol 2006, 7:505–516
4. Yarden Y, Shilo BZ: SnapShot: EGFR signaling pathway. Cell 2007, 131:1018
5. Gotoh N: Feedback inhibitors of the epidermal growth factor receptor signaling pathways. Int J Biochem Cell Biol 2009, 41:511–515
6. Avraham R, Yarden Y: Feedback regulation of EGFR signalling: decision making by early and delayed loops. Nat Rev Mol Cell Biol 2011, 12:104–117
7. Cloughesy TF, Yoshimoto K, Nghiemphu P, Brown K, Dang J, Zhu S, Hsueh T, Chen Y, Wang W, Youngkin D, Liau L, Martin N, Becker D, Bergsneider M, Lai A, Green R, Oglesby T, Koleto M, Trent J, Horvath S, Mischel PS, Mellinghoff IK, Sawyers CL: Antitumor activity of rapamycin in a Phase I trial for patients with recurrent PTEN-deficient glioblastoma. PLoS Med 2008, 5:e8
8. Shtiegman K, Kochupurakkal BS, Zwang Y, Pines G, Starr A, Vexler A, Citri A, Katz M, Lavi S, Ben Basat Y, Benjamin S, Corso S, Gan J, Yosef RB, Giordano S, Yarden Y: Defective ubiquitinylation of EGFR mutants of lung cancer confers prolonged signaling. Oncogene 2007, 26:6968–6978
9. Schneider MR, Werner S, Paus R, Wolf E: Beyond wavy hairs: the epidermal growth factor receptor and its ligands in skin biology and pathology. Am J Pathol 2008, 173:14–24
10. Fitch KR, McGowan KA, van Raamsdonk CD, Fuchs H, Lee D, Puech A, Herault Y, Threadgill DW, Hrabe dA, Barsh GS: Genetics of dark skin in mice. Genes Dev 2003, 17:214–228
11. Vassar R, Fuchs E: Transgenic mice provide new insights into the role of TGF-α during epidermal development and differentiation. Genes Dev 1991, 5:714–727
12. Dominey AM, Wang XJ, King LE Jr, Nanney LB, Gagne TA, Sellheyer K, Bundman DS, Longley MA, Rothnagel JA, Greenhalgh DA, Roop DR: Targeted overexpression of transforming growth factor α in the epidermis of transgenic mice elicits hyperplasia, hyperkeratosis, and spontaneous, squamous papillomas. Cell Growth Differ 1993, 4:1071–1082
13. Cook PW, Piepkorn M, Clegg CH, Plowman GD, DeMay JM, Brown JR, Pittelkow MR: Transgenic expression of the human amphiregulin

gene induces a psoriasis-like phenotype. J Clin Invest 1997, 100:2286–2294
14. Cook PW, Brown JR, Cornell KA, Pittelkow MR: Suprabasal expression of human amphiregulin in the epidermis of transgenic mice induces a severe, early-onset, psoriasis-like skin pathology: expression of amphiregulin in the basal epidermis is also associated with synovitis. Exp Dermatol 2004, 13:347–356
15. Dahlhoff M, Muller AK, Wolf E, Werner S, Schneider MR: Epigen transgenic mice develop enlarged sebaceous glands. J Invest Dermatol 2010, 130:623–626
16. Yuspa SH, Poirier MC: Chemical carcinogenesis: from animal models to molecular models in one decade. Adv Cancer Res 1988, 50:25–70
17. Abel EL, Angel JM, Kiguchi K, Digiovanni J: Multi-stage chemical carcinogenesis in mouse skin: fundamentals and applications. Nat Protoc 2009, 4:1350–1362
18. Nagase H, Mao JH, Balmain A: Allele-specific Hras mutations and genetic alterations at tumor susceptibility loci in skin carcinomas from interspecific hybrid mice. Cancer Res 2003, 63:4849–4853
19. Dahlhoff M, Algul H, Siveke JT, Lesina M, Wanke R, Wartmann T, Halangk W, Schmid RM, Wolf E, Schneider MR: Betacellulin protects from pancreatitis by activating stress-activated protein kinase. Gastroenterology 2010, 138:1585–1594
20. Eisen DB, Michael DJ: Sebaceous lesions and their associated syndromes: part I. J Am Acad Dermatol 2009, 61:549–560
21. Xu Y, Tan LJ, Grachtchouk V, Voorhees JJ, Fisher GJ: Receptor-type protein-tyrosine phosphatase-kappa regulates epidermal growth factor receptor function. J Biol Chem 2005, 280:42694–42700
22. Levkowitz G, Waterman H, Zamir E, Kam Z, Oved S, Langdon WY, Beguinot L, Geiger B, Yarden Y: c-Cbl/Sli-1 regulates endocytic sorting and ubiquitination of the epidermal growth factor receptor. Genes Dev 1998, 12:3663–3674
23. Chin LS, Raynor MC, Wei X, Chen HQ, Li L: Hrs interacts with sorting nexin 1 and regulates degradation of epidermal growth factor receptor. J Biol Chem 2001, 276:7069–7078
24. Gur G, Rubin C, Katz M, Amit I, Citri A, Nilsson J, Amariglio N, Henriksson R, Rechavi G, Hedman H, Wides R, Yarden Y: LRIG1 restricts growth factor signaling by enhancing receptor ubiquitylation and degradation. EMBO J 2004, 23:3270–3281
25. Laederich MB, Funes-Duran M, Yen L, Ingalla E, Wu X, Carraway KL III, Sweeney C: The leucine-rich repeat protein LRIG1 is a negative regulator of ErbB family receptor tyrosine kinases. J Biol Chem 2004, 279:47050–47056
26. Sundberg JP, Sundberg BA, Beamer WG: Comparison of chemical carcinogen skin tumor induction efficacy in inbred, mutant, and hybrid strains of mice: morphologic variations of induced tumors and absence of a papillomavirus cocarcinogen. Mol Carcinog 1997, 20:19–32
27. Zinser GM, Sundberg JP, Welsh J: Vitamin D(3) receptor ablation sensitizes skin to chemically induced tumorigenesis. Carcinogenesis 2002, 23:2103–2109
28. Ito M, Motoyoshi K, Suzuki M, Sato Y: Sebaceous gland hyperplasia on rabbit pinna induced by tetradecane. J Invest Dermatol 1985, 85:249–254
29. Rice JM, Anderson LM: Sebaceous adenomas with associated epidermal hyperplasia and papilloma formation as a major type of tumor induced in mouse skin by high doses of carcinogens. Cancer Lett 1986, 33:295–306

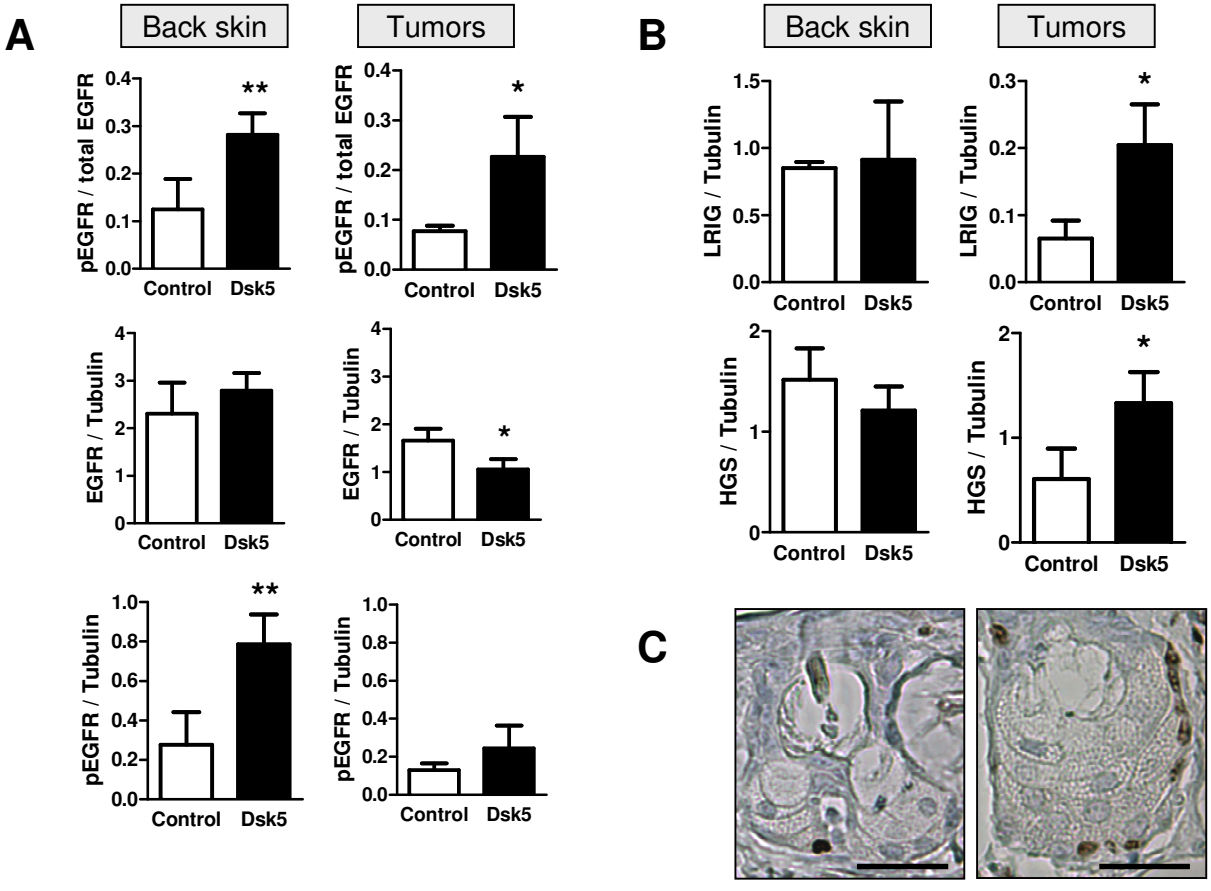
A
Back skin
Tumors
pEGFR / total EGFR
EGFR / Tubulin
pEGFR / Tubulin
Control
Dsk5
B
Back skin
Tumors
LRIG / Tubulin
HGS / Tubulin
C